Study of Submerged Arc Weld Metal and Heat-Affected Zone Microstructures of a Plain Carbon Steel

The nature of microstructures in the subzones of the HAZ greatly influence weld metal toughness and strength

by A. Joarder, S.C. Saha and A.K. Ghose

-- *Reprinted from "WELDING JOURNAL" Volume 70, No. 6, June, 1991*

A detailed study on the microstructure of submerged arc (SA) weld metal and the heat-affected zone of a 1.2-cm (0.5-in.) thick plain carbon steel plate was carried out using transmission electron microscopy. The various subzone microstructure observed in the HAZ of a SA weld are spheroidized, partially transformed, grain-refined and grain-coarsened. The grain-coarsened area exhibits predominantly Widmanstatten ferrite with pearlite, while the other subzones of HAZ reveal polygonal ferrite and pearlite. Depending on the number, size and distribution of inclusions, the weld metal microstructure varies. With a larger number of inclusions, grain boundary ferrite and, in absence of inclusion, either side plate with pearlite or cementite along the boundaries of side plates are observed. It is noticed that a limited number of larger size inclusions favor the formation of acicular ferrite. Because of the prevalence of varying cooling rates in weld metal, a wide range of microsturctures, such as periodic pearlite, grain boundary ferrite with pearlite, and side plate with cementite along the side plate boundaries, are observed.

INTRODUCTION

The microstructures developed in the weld metal (WM) and heat-affected zone (HAZ) of a fusion welding process play an important role in controlling the mechanical properties of weldments. The WM microstructure is controlled mainly by the cooling cycle, while the area adjacent to WM, i.e., the HAZ, exhibits metallurgical transformations due to both heating and cooling cycles. The typical microstructure (Refs. 1-3) of WM in low-carbon low-alloy steels consists of proeutectoid ferrite, Widmanstatten ferrite (side plates), acicular ferrite (AF), bainite and martensite, depending on the cooling rate below A_3 temperature. Dallam, et al. (Ref.4), studied the WM microstructure of low-carbon steel and classified the various microstructures that form in WM. The different microstructural zones (Refs.1,2,5-8) in HAZ are the spheroidized zone, partially transformed zone, grain-refined zone and grain-coarsened zone.

In recent years, there has been an increasing demand for good toughness in the WM of HSLA steels, and considerable interest has been paid to understanding the formation of AF structure because it shows high strength due to its fine grain size (Refs. 9-13). On the other hand, the presence of grain boundary allotriomorphs, Widmanstatten ferrite (WF), bainite and martensite is considered to be detrimental to strength and toughness of the WM. The microstructural variations in the different zones of HAZ, under low-magnification microscope (Refs. 1-8), were studied in detail. But the finer details of microstructures of the WM and HAZ of a plain carbon steel are not fully available in literature (Refs.1,2,6-8), and the data relating to these microstructures are sparse. Therefore, in the present investigation an attempt has been made to study systematically the finer details of WM, as well as HAZ microstructures, of a plain carbon steel weldment by using transmission electron microscopy.

A. Joarder and A.K. Ghose are with the Department of Metallurgical Engineering, Banaras Hindu University, Varanasi, India. S.C. Saha is with the Regional Engineering College, Silchar, Assam, India.

EXPERIMENTAL PROCEDURE

Plain carbon steel plates of 1.2-cm (0.5-in.) thickness were obtained from indigenous sources and bead-on-plate welding on standard plates of 20 x 15 -cm (8 x 6-in.) size was carried out with a mechanized submerged arc welding (SAW) machine. The welding parameters used were: current, 350 A (DC); voltage,

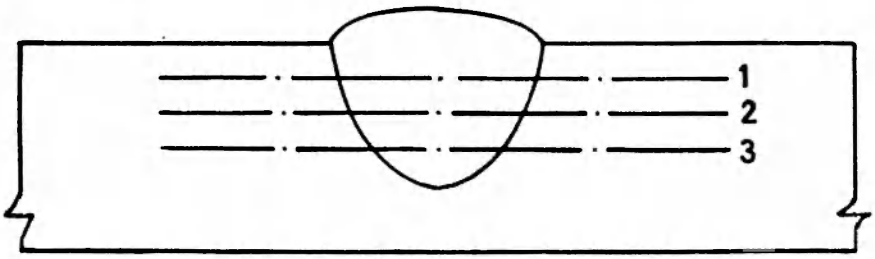

Fig. 1. *Transverse cross-section of a submerged arc weld showing different layers in WM.*

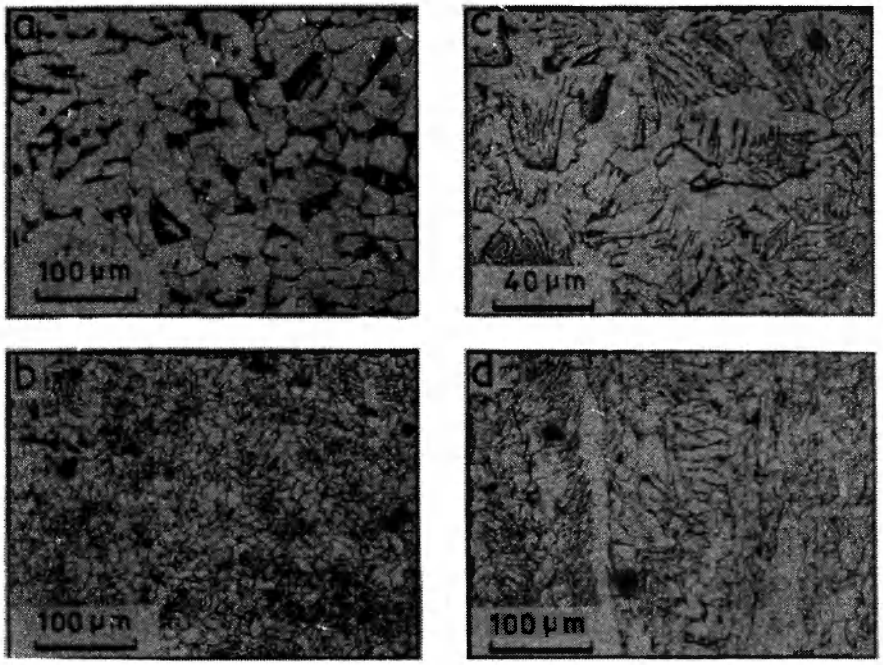

Fig. 2. *Optical micrographs of : A - Base metal: ferrite (white) and pearlite (dark); B - grain-refined HAZ: polygonal ferrite and pearlite; C - grain-coarsened HAZ: WF and pearlite; D - weld metal: (1) grain boundary ferrite, (2) side plate and (3) polygonal ferrite.*

Fig. 3. *TEM of base metal showing ferrite and pearlite*

30 V ; speed of welding, 0.67 cm/s; nozzle angle , 90 deg; and electrode extension, 0.25 cm (0.1 in.). The electrode of IS 7280-1974(AWS EL8K) specification and a diameter of 0.315 cm (0.12 in.) was used with granular basic-type flux. The composition of the steel used was 0.18 C, 0.75 Mn, 0.28 Si, 0.035 S and 0.06 P. Specimens for optical metallography were obtained from the transverse direction of the weld, followed by mechanical polishing by standard technique and etched with 2% nital. Thin foil for transmission electron microscopy were made from thin slices, which were cut with Isomet diamond saw. These slices were taken from three different layers of the weld metal as shown in Fig.1. These were carefully ground to less than 0.1-mm (0.004 -in.) thickness by emery paper. Thin foils were then prepared by a window technique using an electrolyte containing 10% perchloric acid and 90% glacial acetic acid. These foils were examined in a JEOL 200 CX transmission electron microscope at an operating voltage of 160 kV.

RESULTS

Optical Microscopy

The microstructure in the base metal shown in Fig.2A consists of polygonal ferrite (white area) and pearlite (dark area). The HAZ microstructure of grain refined and grain-coarsened areas is shown in Figs. 2B and C, respectively. Comparing with Fig. 2A, it is observed that the grain-refined area exhibits extremely small ferrite grains, clearly indicating that very fine ferrite and pearlite is formed due to the heating and cooling cycles of the SAW process. Figure 2C, representing a grain-coarsened area, exhibits predominantly WF and pearlite. Figure 2D is an optical micrograph taken from the WM area, revealing grain boundary, ferrite, side plate and occasionally equiaxed ferrite. Finer details of the microstructure in the HAZ and WM were studied by TEM.

Transmission Electron Microscopy

An extensive thin-foil transmission electron microscopy (TEM) examination of the HAZ and WM was carried out. The base metal microstructure exhibits ferrite and pearlite, as shown in Fig. 3. The TEMs taken from the HAZ area (Fig. 4A and B) adjacent to the base metal show considerable spheroidization of cementite lamellae in pearlite. Next to the spheroidized

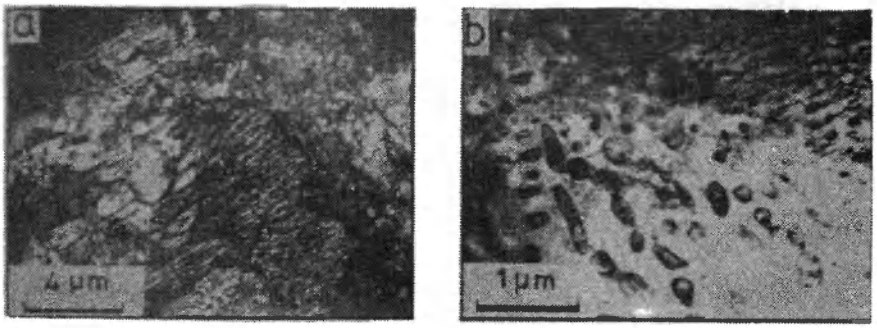

Fig. 4. *TEMs of spheroidized area of HAZ. A - low magnification; B - high magnification clearly showing spheroidized carbide.*

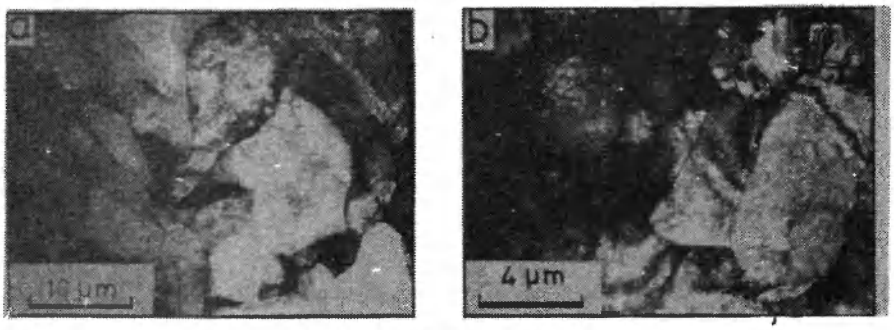

Fig. 5. *TEMs of partially transformed area of HAZ from two different locations. A - low magnification; B - high magnification.*

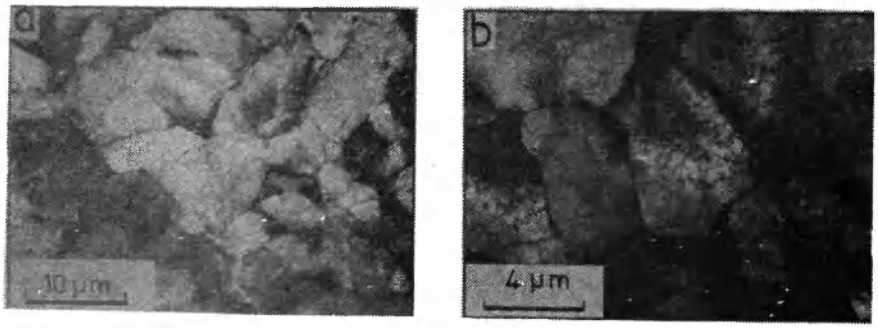

Fig. 6. *TEMs of grain-refined area of HAZ. A - low magnification showing ferrite (white) and pearlite (dark); B - high magnification clearly showing fine pearlite.*

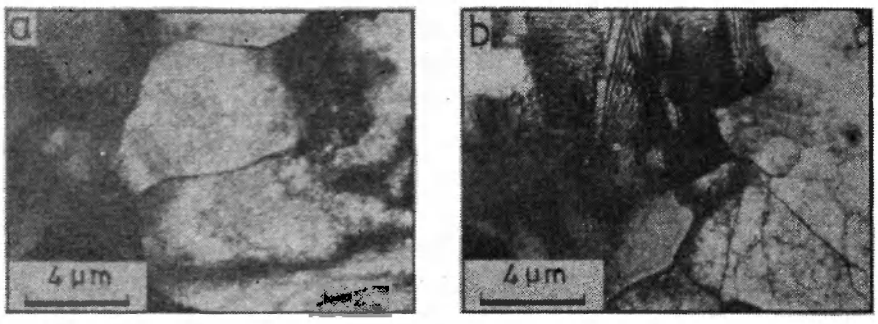

Fig. 7. *TEMs of HAZ. A - transition from fine to coarse grain; B - grain-coarsened structure.*

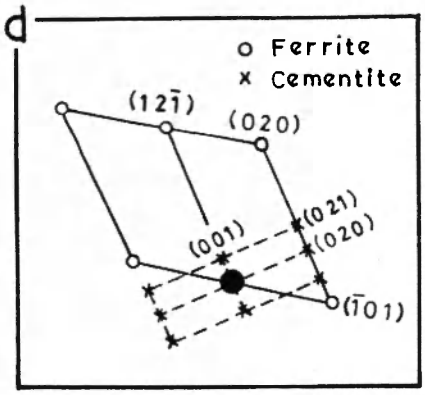

Fig. 8. *TEMs of grain-coarsened HAZ. A - BF; B - DF; C - SAD; D - schematic representation.*

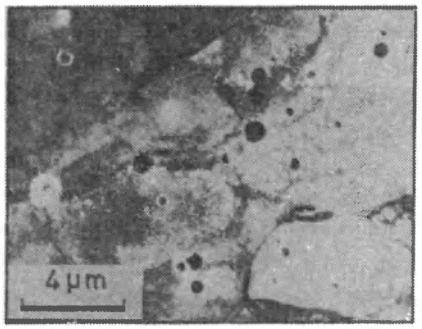

Fig. 9. *TEM of WM (layer 1) showing a large number of inclusions within proeutectoid ferrite*

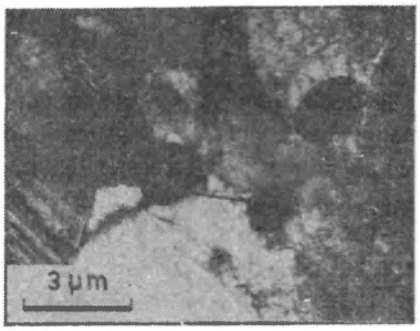

Fig. 10. *TEM of WM (layer 1) showing inclusions along fine ferrite boundaries*

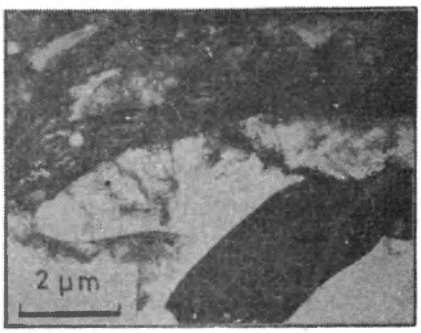

Fig. 11. *TEM of WM (layer 1) showing elongated inclusion*

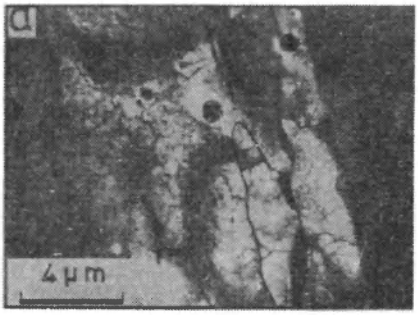

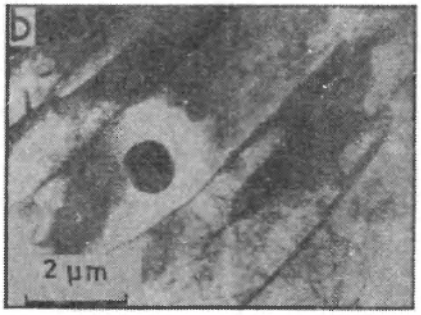

Fig. 12. *TEMs of WM (layer 2) showing acicular ferrite at two different locations. A - low magnification; B - high magnification*

area in the HAZ, the simultaneous presence of fine- as well as coarse-grain structure is observed - Fig. 5A and B. Here pearlite is transformed to austenite during the heating cycle of welding; whereas, during the cooling cycle, the same austenite transforms to fine-grain ferrite and pearlite. This area is designated as a partially transformed region (Refs. 1,2,6). Figure 6A and B shows two TEMs revealing fine-grain microstructure. Both very fine grain ferrite and pearlite are observed in this area as compared to the base metal microstructure - Fig. 3. This clearly indicates that during the heating and cooling cycles a very fine grain structure is formed in the HAZ. This area is generally termed as the grain-refined area (Refs. 1,2,6). Figure 7A reveals both fine and coarse grain, representing the transition of fine to coarse grain, while Fig. 7B reveals coarse grain ferrite and pearlite. Figure 8A and B are bright field (BF) and dark field (DF) micrographs taken from the pearlite area of the grain-coarsened region. A corresponding selected area of diffraction pattern is shown in Fig. 8C, and its schematic representation is shown in Fig. 8D.

Table 1. Phases of Subzones Observed in the HAZ

Subzones	Phases
Partially transformed	Ferrite-pearlite, upper bainite, auto tempered or high-carbon martensite
Grain-refined	Fine-grained ferrite-pearlite
Grain-coarsened	
very fast cooling	Autotempered martensite, lower bainite, martensite
fast cooling	Massive ferrite with either Fe_3C or austenite between fingers of ferrite
medium high cooling	Periodic pearlite
medium slow cooling	WF and pearlite
slow cooling	Ferrite-pearlite

Assuming a varying inclusion content at different levels in SA welds, transmission electron microscopy of the WM was carried out at different areas as shown in Fig. 1. Figure 9 is a TEM of area "1" revealing a large number of inclusions of varying sizes (0.2-0.7 µm) within the ferrite, while Figs. 10 and 11 show inclusions along the grain boundaries of fine-grain ferrite. This demonstrates that these inclusions inhibit grain coarsening. Occasionally, an elongated inclusion is also observed as shown in Fig. 11. But most of the inclusions observed in TEMs are spherical in shape. Figure 12A and B shows fine irregular-shaped (neither polygonal nor equiaxed) ferrite along with inclusions. This type of ferrite is AF. Inclusions play an important role in the formation of this type of ferrite, mainly acting as nucleation sites (Refs. 14-19). It is also observed from the TEMs that the formation of AF is favorable when a reasonable number of inclusions are present in the WM. In this study, area "2" exhibits the presence of AF, but pearlite is not observed in the surrounding area of the AF.

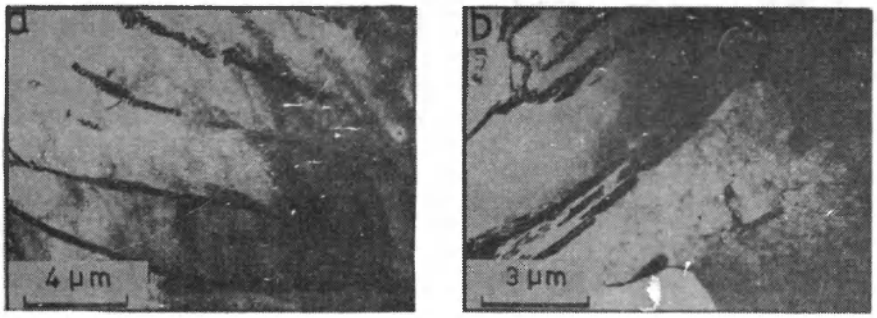

Fig. 13. *TEMs of WM (layer 3) from two different locations. A - side plates with pearlite and/or cementite along the side plate boundaries; B - secondary side plates and cementite along the plate boundaries*

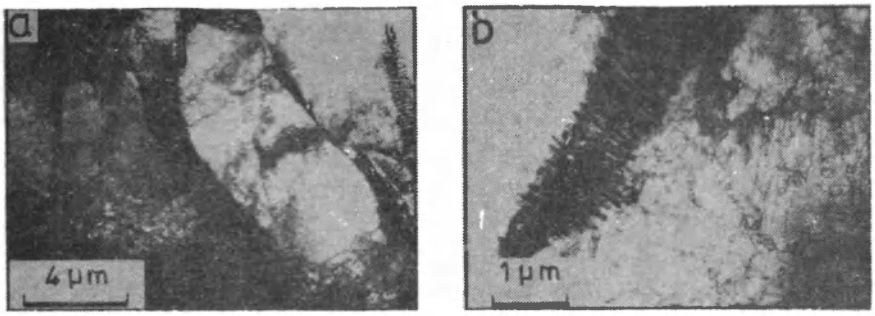

Fig. 14. *TEMs of WM (layer 3). A - ferrite and pearlite; B - pearlite at higher magnification of A*

TEMs of area "3" of the WM (devoid of inclusions) exhibit either side plate (Fig. 13A, B) or grain boundary ferrite with pearlite (Fig. 14) or cementite along the side plate boundaries - Fig. 13A. At times, periodic pearlite is observed - Fig. 15.

DISCUSSION

The results of the present investigation of HAZ reveal the presence of various subzones, namely spheroidized carbide, partially transformed, fine-grained, transition of fine- to coarse-grain and grain-coarsened area (starting from base to weld metal sides). The TEMs of base metal and HAZ areas primarily exhibit equiaxed ferrite and pearlite. However, the grain-coarsened HAZ area reveals predominantly WF. These subzones are in agreement with low magnification micrographs reported by Smith, et al. (Ref. 5), and other investigators (Refs.1,2,6). Rasanen and Tenkula (Ref. 6), however, investigated the details of these subzones produced under simulated conditions of varying cooling rates and discussed their TEMs on the basis of theoretical physical metallurgy. According to them (depending on the rate of cooling), these subzones may have the phases listed in Table 1. It is observed from the TEMs in the present study that subzones of partially transformed (Fig. 5), grain-refined (Fig. 6) and grain-coarsened regions (Fig. 7B) of the HAZ in

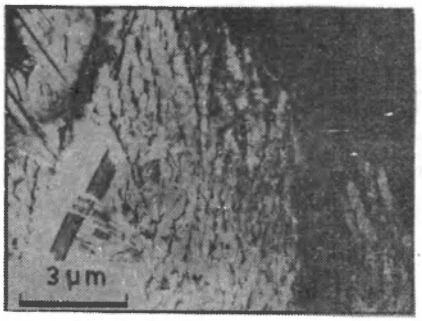

Fig. 15. *TEM of WM (layer 3) showing periodic pearlite*

the SAW weldment (which is a slow cooling process) are in agreement with the results of Rasanen and Tenkula (Ref. 6).

The WM microstructures at different locations consist mainly of WF, AF and proeutectoid ferrite. It is well established (Refs. 3, 14-19) that oxide inclusions play an important role in the formation of AF. During this investigation, it was observed that although inclusions favor the formation of AF (Fig. 12), a large number of inclusions favor the formation of proeutectoid ferrite - Fig. 9.

It is well documented (Refs. 20-23) that the oxygen level of SA welds affects the WM microstructure. According to Abson, et. al. (Ref. 20), coarse-grain bainite structure is formed with 0.01% oxygen; whereas, fine AF is formed if oxygen is 0.025%. Cochrane and Kirkwood (Ref. 21), however, report that the SAW process with manganese silicate fluxes and a high oxygen level (>0.07%) lead to a large number of inclusions at the austenite boundary, which helps in early nucleation of ferrite. This results in a lamellar structure rather than AF since the earlier nucleated side plates grow rapidly across the austenite grains. Abson and Dolby (Ref. 22) also mention that oxygen content of WM to some extent affects the amount of AF formed. They further indicate that too low oxide inclusions lead to bainitic structure; whereas, a large number of oxide inclusions favor proeutectoid ferrite nucleation. Brownlee, et al. (Ref. 23), studied the formation of AF in a series of bead-on-plate SA welds with a systematic variation of aluminum and titanium in the WM. They report that increasing aluminum concentration increases AF, but after a critical limit (>0.25 wt-%), the volume-percent of AF decreases continuously. They also mention that maximum AF volume fraction is associated with a high

density of inclusions within a critical size range of approximately 0.5 μm. In the present investigation, it is observed that a large number of small inclusions with varying sizes (0.2-0.7 μm) results in the formation of proeutectoid ferrite; whereas, larger inclusions only favor nucleation of AF. These observations are in agreement with the results reported by Brownlee, et al. (Ref. 23). Thus, it may be concluded from the present investigation as well as from earlier reported investigations (Refs. 20-23), that an adequate number and appropriate dispersion of inclusions are an essential requirement for the nucleation of AF.

Yamamoto, et al. (Ref. 24), report that oxide inclusions not only favor the formation of AF, but they also help in controlling grain coarsening. This inhibition of grain coarsening by oxides is similar to the presence of nitride and carbide in steel, but the oxides are more effective in the welding process as they have greater thermal stability. Fleck, et al. (Ref. 25), as well as Liu and Olson (Ref. 15), also suggest that oxide (oxy-sulfide) inclusions restrict the growth of austenite grains. The present study clearly shows the inhibition of grain coarsening when inclusions segregate along the grain boundaries - Fig. 10. This is consistent with the observation of Yamamoto, et al. (Ref. 24).

Dallam, et al. (Ref. 4.), investigated the microstructural variation of Nb microalloyed steel with the oxygen content in SA welds, using a CaF_2-CaO-SiO_2 flux system of varying composition. They observed that 380 ppm oxygen in the weld metal a mixed microstructure of grain boundary ferrite with AF is obtained; whereas, at 260 and 107 ppm of oxygen, predominantly AF and bainitic structures are obtained, respectively. It is further indicated by them that 90% AF in the weld metal for the above flux system is obtained when the oxygen content is in the range of 200 to 250 ppm. Keeping the above observations in view, the present investigation took thin slices for TEM studies from three different layers of the WM, as shown in Fig. 1. The TEMs clearly indicate that layer 1 exhibits a large number of inclusions, resulting in the formation of grain boundary ferrite (Fig. 9), while layer 2, with a relatively less number of inclusions favors AF formation - Fig. 12. On the other hand, layer 3 evidences predominantly WF (side plates) with pearlite and/or cementite along the boundaries of the side plates - Fig. 13. This clearly suggests that side plate-type morphology is formed in that portion of WM that is free from inclusions. Since the presence of grain boundary and side plate ferrite are detrimental to toughness, the presence of AF throughout the cross-section of WM is desirable to obtain better toughness and strength. This may be achieved either by uniformly distributing the inclusions through controlled weld pool stirring (Ref. 26), inoculation (Refs. 27,28), arc oscillation and arc pulsation (Ref. 29) (commonly used for grain refining); or by introducing oxide-forming elements like aluminum (Ref. 23), titanium (Ref. 23), titanium-boron (Ref. 25), etc., along with the welding wire or by addition of these elements in the steel (Refs. 24,30).

Different varieties of Widmanstatten morphologies can be obtained, depending upon the degree of supersaturation. Dube, et al. (Ref. 31), classified these morphologies, which are further detailed by Aaronson (Ref. 32). These morphologies are primary side plates and intragranular plates. The formation and mechanism of the commonly occurring secondary side plates in plain carbon steels have been detailed by Townsend and Kirkaldy (Ref. 33). In the present investigation, these secondary plates are observed in Figs. 2D (low magnification) and 13 (finer details). The latter figure not only reveals the side plates with pearlite, but also exhibits cementite along the side plate boundaries.

Postsolidification phase transformation in WM at different areas reveals different microstructures. This is due to the complicated nature of weld pool solidification, which is affected by various factors such as: plate and weld pool geometry, its physical properties, welding process, and boundary conditions. This naturally leads to various degrees of cooling rates at different locations in the weldmetal. Rasanen and Tenkula report that, depending on the cooling rates, different structures are formed such as periodic pearlite, WF and pearlite and ferrite pearlite. These microconstituents are also observed in the present investigation as shown in Figs. 15, 13 and 14, respectively. The precipitation of cementite along the side plate boundaries observed in the present study (Fig. 13A) seems to be similar to bainitic structure (i.e., upper bainite consisting of ferrite laths with cementite along lath boundaries - Refs. 34, 35).

Strangwood and Bhadeshia (Refs. 19,36) report that the growth of AF is diffusionless and is formed by a displacement transformation mechanism. Sugden and Bhadeshia (Ref. 17) propose that a AF formation mechanism is similar to bainite transformation; however, the morphology of AF is different, since it nucleates intragranularly from point sites. The results of the present study reveal an absence of pearlite in the surrounding area of AF, as in Fig. 12A, B. Thus, it appears from the present investigation that diffusionless shear-type (similar to martensite formation) transformation is the mechanism of formation of AF in accordance with other investigators (Refs. 19,36).

Conclusions

The microstructure of a single-pass SAW weld in plain carbon steel was investigated with a transmission electron microscope. The following conclusions are drawn:

The microstructures of the HAZ exhibit different subzones; spheroidized, partially transformed, grain-refined, transition of fine to coarse-grain and grain-coarsened area, as observed from the base metal side.

The HAZ microstructure in the partially transformed and the grain-refined areas reveal ferrite and pearlite, while the grain-coarsened area shows predominantly Widmanstatten ferrite and pearlite.

The top, middle and base of the weld metal reveal different types of microstructure:

Top - Exhibits grain-boundary ferrite, with a larger number of inclusions within the ferrite and also along the grain boundaries (sometimes restricting the growth of ferrite grains).

Middle - Exhibits relatively fewer inclusions, which favor the formation of acicular ferrite.

Base - Exhibits the absence of inclusions and favors a side plate morphology with pearlite or cementite along the side plate boundaries. Grain boundary ferrite is also observed.

A limited number of larger inclusions help in the formation of acicular ferrite; whereas, a large number of smaller (0.2 - 0.7 μm) inclusions favor grain boundary ferrite formation.

Acknowledgments

The authors wish to thank the Department of Metallurgical Engineering, Banaras Hindu University, for the provision of laboratory facilities to carry out the investigation. Ashok Joarder wishes to thank the Council of Scientific and Industrial Research (CSIR) for a research associateship.

References

1. Kou s. 1987. Welding Metallurgy. Wiley Interscience Pub., New York, N.Y.
2. Easterling, K.E. 1983. Introduction to the Physical Metallurgy of Welding. Butterworths & Co., London, England.
3. Dolby, R.E. 1983. Advances in welding metallurgy of steel. Metals Technology 10(9): 349-362.
4. Dallam, C.B., Liu, S., and Olson, D.L. 1985. Flux composition dependence of microstructure and toughness of submerged arc HSLA weldments. Welding Journal 64(5): 140-s to 151-s.
5. Smith, E., Coward, M.D., and Apps, R.L. 1970. Weld heat-affected zone structure and properties of two mild steels. Welding Met. Fabr. 38:242-251.
6. Rasanen, E., and Tenkula, J. 1972. Phase changes in the welded joints of constructional steels. Scand. Journal of Metallurgy 1:75-80.
7. Gooch T.G., and Hart, P.H.M. 1986. Solid-state phase transformations in steel during welding. Proc. Intl. Conf. on Trends in Welding Research, Gatlinburg, Tenn., ASM Intl., Ed. S.A. David, pp. 161-176.
8. Easterling, K.E. 1986. Predicting heat-af-fected zone microstructures and properties in fusion welds. Proc. Intl. Conf. on Trends in Welding Research, Gatlinburg, Tenn., ASM Intl., Ed. S.A. David, pp. 177-185.
9. Dolby, R.E. 1976. Factors controlling weld toughness - the present position. part II - weld metal. The Welding Institute, Cambridge, England.
10. Glover, A.G., McGarth,J.T., Tinkler, M.J., and Weatherly, G.C. 1977. The influence of cooling rate and composition on weld metal microstructure in C-Mn HSLA steel. Welding Journal 56(9):267-s to 273-s.
11. Glover, A.G., McGarth, J.T., and Eaton, N.F. 1977. Symposium on Toughness Characterization and Specifications for HSLA and Structural Steels. Metallurgical Society of AIME, Atlanta, Ga., pp. 143 to 160.
12. Groug, O., and Matlock, D.R. 1986. Microstructural development in mild and low-alloy steel weld metals. Intl. Metals Review 31(1):27-48.
13. Abson, D.J., and Pargeter, R.J. 1986. Factors influencing as-deposited strength, microstructure and toughness of manual metal arc welds suitable for C-Mn steel fabrications. Intl. Metals Review 31(1): 141-194.
14. Dowling, J.M., Corbett, J.M., and Kerr, H.W. 1986. Inclusion phases and the nucleation of acicular ferrite in submerged arc welds in HSLA steel. Metallurgical Transactions 17A(9): 1611-1623.
15. Liu S., and Olson, D.L. 1986. The role of inclusions in controlling HSLA steel weld microstructures. Welding Journal 65(6):139-s to 149-s.
16. Barbaro, F.J., Krauklis, P., and Easterling, K.E. 1989. Formation of acicular ferrite at oxide particles in steels. Material Science and Technology 5(11): 1057-1068.
17. Sugden, A.A.B., and Bhadeshia, H.K.D.H. 1989. Lower acicular ferrite. Metallurgical Transactions 20A(9): 1811-1818.
18. Yang, J.R., and Bhadeshia, H.K.D.H. 1986. Thermodynamics of the acicular ferrite transformation in alloy steel weld deposits. Proc. In tl. Conf. on Trends in Welding Research. Gatlinburg, Tenn., ASM Intl., Ed.S.A. David, pp. 161-176.
19. Strangwood, M., and Bhadeshia, H.K.D.H. 1986. The mechanism of acicular ferrite formation in steel weld deposits, ibid, pp. 209-213.
20. Abson, D.J., Dolby, R.E., and Hart, P.H.M. 1978. The role of nonmetallic inclusions in ferrite nucleation in carbon steel weld metals. Proc. Intl. Conf. on Trends in Steels and Consumables for Welding, London, England, The Welding Institute, pp.75-101.
21. Cochrane, R.C., and Kirkwood, P.R. 1978. The effect of oxygen on weld metal microstructure. ibid, pp. 103-121.
22. Abson, D.J. and Dolby, R.E. 1978. Welding Institute Research Bulletin, pp. 202-206.
23. Brownlee, J.K., Matlock, D.K., and Edwards, G.R. 1986. Effect of aluminum and titanium on the microstructure and properties of microalloyed steel weld metal. ibid, pp. 245-250.
24. Yamamoto, K., Matsuda, S., Haze, T., Chijiiwa, R., and Mimura, H. 1987. Proc Symp. Residual and Unspecified Elements in Steels. Bal Harbour, Fl, ASTM.
25. Fleck, N.A., Grong, O., Edwards, G.R., and Matlock, D.K. 1986. The role of filler metal wire and flux composition in submerged arc weld metal transformation kinetics. Welding Journal 65(5): 113-s to 121-s.
26. Venkatraman, S., Devletian, J.H., Wood, W.E., and Atteridge, D.G. 1983. Grain refinement in casting welds. Conf. Pro. AIME, Ed. Abbachain, p. 275.

Contd. to P.177

NDT

SPOTCHECK®

Shows what you are missing.

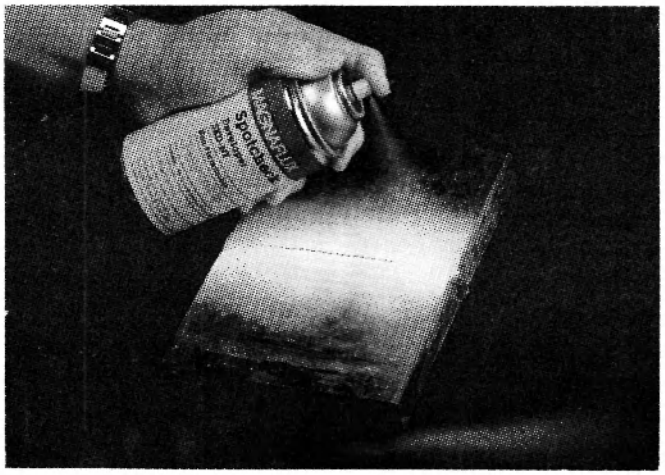

The dye penetrant testing system that more than meets "minimum code requirements".

SPOTCHECK visible dye penetrant has superior capillary action with the proven ability to seep into the tightest surface discontinuities. Its vivid red colour provides the brightest contrast to bring to light flaws and cracks as small as 2 micron × 20 micron deep. **A proven fact which conventional competitive products don't even come close to meeting.** With such performance, you can be sure that time and again, your NDT code specifications are surely met. Consistently!

More economy, more convenience

SPOTCHECK products are formulated to have the lowest surface tension for superior surface 'wettability', thereby ensuring that only the thinnest possible film is needed to do the job. **Greater surface area coverage - greater economy in use.**

SPOTCHECK comes in handy aerosol cans (400 ml.can capacity) for 'in-situ' applications. The special SPOTCHECK formulations matched with time tested aerosol valve and gasketing materials ensures fail-proof, non-clogging performance, till the can is completely exhausted. No more throwing away half-used cans. **No wastage - more economy for you.**

All these and more, have won SPOTCHECK approvals to the most critical and stringent specifications like MIL-STDS., ASME, B& PV Code, ASTM, NAVSEA, BS and NPC (nuclear specifications for low sulphur & chlorine).

This international quality product is now brought to you in India in collaboration with MAGNAFLUX Corp., USA.

For further details write to:

NAGARJUNA SIGNODE LIMITED

(Quality Assurance Products Group)
401 & 402, New Udyog Mandir, Mogul Lane, Malum, Bombay-400 016
Phone: 461652/456493. Tlx: 011-73838

Regd. Office: Nagarjuna Hills, Punjagutta, Hyderabad-500 482 India.
Phone: 35829/225277. Telex: 0425-6754 NSG IN Fax: 91-842-229629. New Delhi: 6442344 Madras: 654893
Calcutta: 347352 Bangalore: 234017 Rourkela: 5642 Jamshedpur: 27974 Bokaro: 7336 Bhilai: 2172.

MAGNAFLUX®